FLAVODIIRON2 and FLAVODIIRON4 Proteins Mediate an Oxygen-Dependent Alternative Electron Flow in Synechocystis sp PCC 6803 under CO2-Limited Conditions

Shimakawa, Ginga ; Shaku, Keiichiro ; Nishi, Akiko ; Hayashi, Ryosuke ; Yamamoto, Hiroshi ; Sakamoto, Katsuhiko ; Makino, Amane ; Miyake,…

(Citation)
Plant Physiology,167(2):472-480

(Issue Date)
2015-02

(Resource Type)
journal article

(Version)
Version of Record

(URL)
https://hdl.handle.net/20.500.14094/90003821

FLAVODIIRON2 and FLAVODIIRON4 Proteins Mediate an Oxygen-Dependent Alternative Electron Flow in *Synechocystis* sp. PCC 6803 under CO_2-Limited Conditions[1][OPEN]

Ginga Shimakawa, Keiichiro Shaku, Akiko Nishi, Ryosuke Hayashi, Hiroshi Yamamoto, Katsuhiko Sakamoto, Amane Makino, and Chikahiro Miyake*

Department of Biological and Environmental Science, Faculty of Agriculture, Graduate School of Agricultural Science, Kobe University, Nada, Kobe 657–8501, Japan (G.S., K.Sh., A.N., R.H., K.Sa., C.M.); Department of Botany, Graduate School of Science, Kyoto University, Sakyo-ku, Kyoto 606–8502, Japan (H.Y.); Department of Agriculture, Graduate School of Agricultural Science, Tohoku University, Tsutsumidori-Amamiyamachi, Aoba-ku, Sendai 981–8555, Japan (A.M.); and Core Research for Evolutional Science and Technology, Japan Science and Technology Agency, Chiyoda-ku, Tokyo 102–0076, Japan (A.M., C.M.)

This study aims to elucidate the molecular mechanism of an alternative electron flow (AEF) functioning under suppressed (CO_2-limited) photosynthesis in the cyanobacterium *Synechocystis* sp. PCC 6803. Photosynthetic linear electron flow, evaluated as the quantum yield of photosystem II [Y(II)], reaches a maximum shortly after the onset of actinic illumination. Thereafter, Y(II) transiently decreases concomitantly with a decrease in the photosynthetic oxygen evolution rate and then recovers to a rate that is close to the initial maximum. These results show that CO_2 limitation suppresses photosynthesis and induces AEF. In contrast to the wild type, *Synechocystis* sp. PCC 6803 mutants deficient in the genes encoding FLAVODIIRON2 (FLV2) and FLV4 proteins show no recovery of Y(II) after prolonged illumination. However, *Synechocystis* sp. PCC 6803 mutants deficient in genes encoding proteins functioning in photorespiration show AEF activity similar to the wild type. In contrast to *Synechocystis* sp. PCC 6803, the cyanobacterium *Synechococcus elongatus* PCC 7942 has no FLV proteins with high homology to FLV2 and FLV4 in *Synechocystis* sp. PCC 6803. This lack of FLV2/4 may explain why AEF is not induced under CO_2-limited photosynthesis in *S. elongatus* PCC 7942. As the glutathione *S*-transferase fusion protein overexpressed in *Escherichia coli* exhibits NADH-dependent oxygen reduction to water, we suggest that FLV2 and FLV4 mediate oxygen-dependent AEF in *Synechocystis* sp. PCC 6803 when electron acceptors such as CO_2 are not available.

In photosynthesis, photon energy absorbed by PSI and PSII in thylakoid membranes oxidizes the reaction center chlorophylls (Chls), P700 in PSI and P680 in PSII, and drives the photosynthetic electron transport (PET) system. In PSII, water is oxidized to oxygen as the oxidized P680 accepts electrons from water. These electrons then reduce the cytochrome b_6/f complex through plastoquinone (PQ) in the thylakoid membranes. Photooxidized P700 in PSI accepts electrons from the reduced cytochrome b_6/f complex through plastocyanin or cytochrome c_6. Electrons released in the photooxidation of P700 are used to produce NADPH through ferredoxin and ferredoxin $NADP^+$ reductase. Thus, electrons flow from water to NADPH in the so-called photosynthetic linear electron flow (LEF). Importantly, LEF induces a proton gradient across the thylakoid membranes, which provides the driving force for ATP production by ATP synthases in the thylakoid membranes. NADPH and ATP serve as chemical energy donors in the photosynthetic carbon reduction cycle (Calvin cycle).

It recently has been proposed that, in cyanobacteria, the photorespiratory carbon oxidation cycle (photorespiration) functions simultaneously with the Calvin cycle to recover carbon for the regeneration of ribulose-1,5-bisphosphate, one of the substrates of Rubisco (Hagemann et al., 2013). Rubisco catalyzes the primary reactions of carbon reduction as well as oxidation cycles. However, the presence of a specific carbon concentration mechanism (CCM) in cyanobacteria had been thought to prevent the operation of photorespiration. CCM maintains a high concentration of CO_2 around Rubisco so that the oxygenase activity of Rubisco is suppressed (Badger and Price, 1992). However, recent studies on mutants deficient in

[1] This work was supported by the Japan Society for the Promotion of Science (Scientific Research grant no. 21570041 to C.M.) and the Ministry of Education, Culture, Sports, Science, and Technology in Japan (Scientific Research on Innovative Areas grant no. 22114512 to C.M. and A.M.).

* Address correspondence to cmiyake@hawk.kobe-u.ac.jp.

The author responsible for distribution of materials integral to the findings presented in this article in accordance with the policy described in the Instructions for Authors (www.plantphysiol.org) is: Chikahiro Miyake (cmiyake@hawk.kobe-u.ac.jp).

[OPEN] Articles can be viewed without a subscription.

www.plantphysiol.org/cgi/doi/10.1104/pp.114.249987

photorespiration enzymes have shown that photorespiration functions, particularly under CO_2-limited conditions, in cyanobacteria as it does in higher plants (Eisenhut et al., 2006, 2008).

Decreased consumption of NADPH under CO_2-limited or high-light conditions causes electrons to accumulate in the PET system. As a result, the photooxidation and photoreduction cycles of the reaction center Chls in PSI and PSII become uncoupled from the production of NADPH, inducing alternative electron flow (AEF) pathways (Mullineaux, 2014). In cyanobacteria, several AEFs that differ from those in higher plants are proposed to function as electron sinks (Mullineaux, 2014). Electrons accumulated in the PET system flow to oxygen through FLAVODIIRON1 (FLV1) and FLV3 proteins in PSI and the terminal oxidase, cytochrome *c* oxidase complex, and cytochrome *bd*-quinol oxidase (Pils and Schmetterer, 2001; Berry et al., 2002; Helman et al., 2003; Nomura et al., 2006; Lea-Smith et al., 2013). Cyanobacterial FLV comprises a diiron center, a flavodoxin domain with an FMN-binding site, and a flavin reductase domain (Vicente et al., 2002). In *Synechocystis* sp. PCC 6803, Helman et al. (2003) identified four genes encoding FLV1 to FLV4 and showed that FLV1 and FLV3 were essential for the photoreduction of oxygen by PSI. FLV1 and FLV3 were proposed to function as a heterodimer (Allahverdiyeva et al., 2013). FLV2/4 have been proposed to function in energy dissipation associated with PSII (Zhang et al., 2012). In addition, hydrogenases convert H^+ to H_2 with NADPH as an electron donor (Appel et al., 2000). Furthermore, Flores et al. (2005) suggested that the nitrate assimilation pathway functions in AEF when the cells live in medium containing nitrate.

To elucidate the physiological functions of these AEFs, evaluation of the presence and capacity of each AEF pathway is required. Therefore, in vivo analyses of electron fluxes are essential. We had found that an electron flow uncoupled from photosynthetic oxygen evolution functioned under suppressed (CO_2-limited) photosynthesis in the cyanobacterium *Synechocystis* sp. PCC 6803 but not in *Synechococcus elongatus* PCC 7942 (Hayashi et al., 2014), indicating that an AEF operated in *Synechocystis* sp. PCC 6803. This AEF was induced in high-[CO_2]-grown *Synechocystis* sp. PCC 6803 during the transition from CO_2-saturated photosynthesis to CO_2-limited photosynthesis (Hayashi et al., 2014). In contrast, in *Synechocystis* sp. PCC 6803 grown at ambient CO_2 concentration, AEF was detected immediately following the transition to CO_2-limited photosynthesis (Hayashi et al., 2014), suggesting that AEF was already induced under ambient atmospheric conditions.

The expression of the AEF activity observed under CO_2-limited photosynthesis required the presence of oxygen in *Synechocystis* sp. PCC 6803 (Hayashi et al., 2014). In *Synechocystis* sp. PCC 6803, FLV1/3 were proposed to catalyze the photoreduction of oxygen (Helman et al., 2003). However, Hayashi et al. (2014) found no evidence that FLV1/3 operated under CO_2-limited photosynthesis: a mutant *Synechocystis* sp. PCC 6803 deficient in FLV1/3 maintained almost constant electron flux under CO_2-limited photosynthesis after the transition from CO_2-saturated conditions. Thus, the postulated photoreduction of oxygen by FLV1/3 was not responsible for the electron flux observed under CO_2-limited photosynthesis in *Synechocystis* sp. PCC 6803.

In this study, we aimed to elucidate the molecular mechanism of the oxygen-dependent AEF functioning under CO_2-limited photosynthesis in *Synechocystis* sp. PCC 6803. The possibility that FLV2 and FLV4 catalyze the photoreduction of oxygen under CO_2-limited photosynthesis could not be excluded, given that AEF in high-[CO_2]-grown *Synechocystis* sp. PCC 6803 was induced following the transition to CO_2-limited photosynthesis (Hayashi et al., 2014). Both FLV2 and FLV4 are predicted to possess oxidoreductase motifs, similar to FLV1 and FLV3 (Helman et al., 2003; Zhang et al., 2012). Furthermore, the expression of two FLV genes (*flv2* and *flv4*) was enhanced under low-[CO_2] conditions (Zhang et al., 2009). Zhang et al. (2012) proposed that FLV2 and FLV4 did not donate electrons to oxygen on the basis of the finding that the *Synechocystis* sp. PCC 6803 mutants deficient in FLV1/3 showed no light-dependent oxygen uptake (Helman et al., 2003). However, Helman et al. (2003) cultivated *Synechocystis* sp. PCC 6803 strains deficient in FLV1 and FLV3 proteins under high-[CO_2] conditions, and we cannot exclude the possibility that the FLV2 and FLV4 proteins were not produced in the studied cells. Taken together, it seems plausible that FLV2 and FLV4 mediate oxygen-dependent AEF following the transition to CO_2-limited photosynthesis. To evaluate this possibility, we constructed *Synechocystis* sp. PCC 6803 mutants deficient in *flv2* and *flv4* and measured their oxygen evolution and Chl fluorescence simultaneously. The mutants showed suppressed LEF after transition to CO_2-limited photosynthesis, similar to *S. elongatus* PCC 7942. We also tested the possibility that photorespiration functions as an electron sink under CO_2-limited photosynthesis in *Synechocystis* sp. PCC 6803. A recent study revealed photorespiratory oxygen uptake in a *flv1/3* mutant under CO_2-depleted conditions (Allahverdiyeva et al., 2011). In this study, we found that the quantum yield of photosystem II [Y(II)] of mutants deficient in genes encoding proteins that function in photorespiration was similar to that of wild-type *Synechocystis* sp. PCC 6803. Thus, FLV2 and FLV4 appear to function in the oxygen-dependent AEF under CO_2-limited photosynthesis in *Synechocystis* sp. PCC 6803. This inference is further supported by the lack of FLV2 and FLV4 homologs in the genome of *S. elongatus* PCC 7942 (Bersanini et al., 2014). In addition, we found oxygen-reducing activities of recombinant glutathione *S*-transferase (GST)-FLV4 fusion protein, similar to those of recombinant FLV3 protein (Vicente et al., 2002). In light of these results, we discuss the molecular mechanism of the oxygen-dependent AEF under CO_2-limited photosynthesis and the physiological function of FLV proteins in *Synechocystis* sp. PCC 6803.

RESULTS

FLV2 and FLV4 Are Essential for AEF under CO_2-Limited Photosynthesis in *Synechocystis* sp. PCC 6803

We monitored Chl fluorescence and the concentration of oxygen in medium containing *Synechocystis* sp. PCC 6803 and *S. elongatus* PCC 7942 cells (Fig. 1). During the measurements, the top of the reaction chamber was open to allow equilibration of the medium with air. Cyanobacteria were added after oxygen concentration in the medium had equilibrated with the concentration in air (about 250 μM at 25°C) in the dark. With both of the cyanobacterial strains (compare Fig. 1, A and C), the medium oxygen concentration quickly declined to a lower equilibrium due to respiratory oxygen consumption. Upon illumination with actinic light (200 μmol photons m^{-2} s^{-1}), the relative Chl fluorescence increased from minimum to steady state and then decreased transiently (Fig. 1, A and C), while the electron flux in PSII [Y(II) = $(F_m' - F_s)/F_m'$, where F_m' = maximum variable fluorescence and F_s = steady-state fluorescence under actinic light] was high (Fig. 1, B and D). Actinic light started photosynthesis as indicated by the increase in oxygen concentration in the medium (Fig. 1, A and C). In both strains, medium oxygen concentration reached a peak when F_s had started to increase; F_s continued to rise while Y(II) decreased and oxygen concentration shifted toward a lower equilibrium (*Synechocystis* sp. PCC 6803, Fig. 1, A and B; *S. elongatus* PCC 7942, Fig. 1, C and D). Thereafter, the parameters developed differently in the two strains. F_s decreased continuously, paralleled by an increasing Y(II) in *Synechocystis* sp. PCC 6803 (Fig. 1, A and B). In contrast, F_s and Y(II) remained at high and low levels, respectively, in *S. elongatus* PCC 7942 (Fig. 1, C and D). Addition of CO_2 (as $NaHCO_3$) caused an increase in medium oxygen concentration and a decrease in F_s in both strains (Fig. 1, A and C) as well as a sharp increase of Y(II) in *S. elongatus* PCC 7942 (Fig. 1D). In separate experiments, we determined oxygen evolution rates at the three times marked in Figure 1 as α (CO_2 in the medium not yet depleted by photosynthesis), β (medium CO_2 at a low steady state controlled by

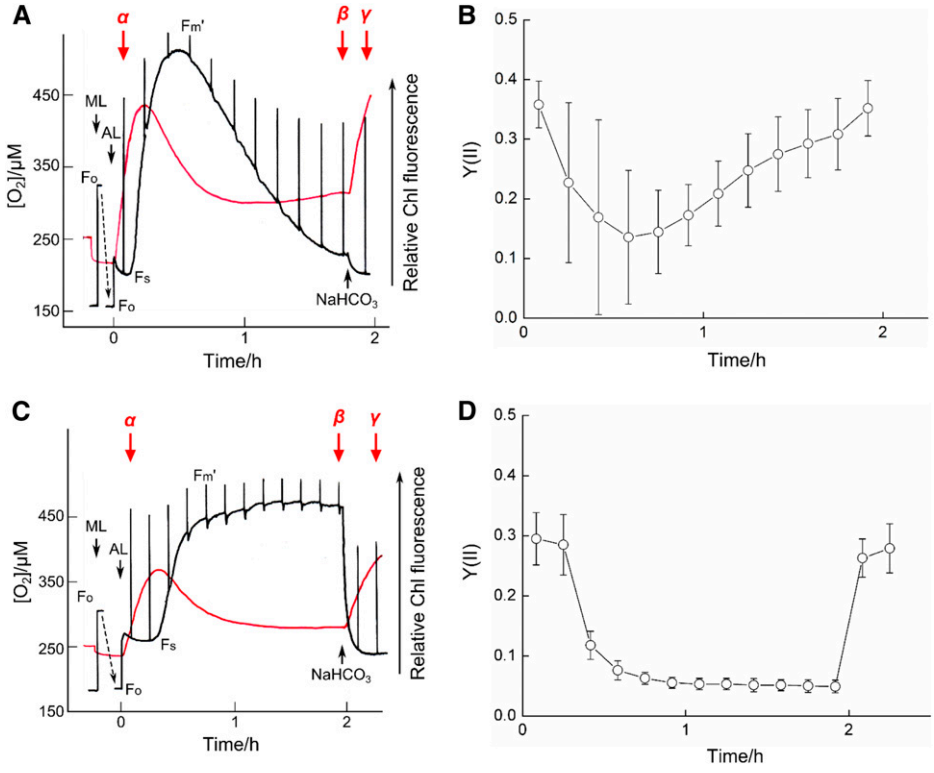

Figure 1. Development of photosynthetic parameters in media containing high-[CO_2]-grown *Synechocystis* sp. PCC 6803 (A and B) and *S. elongatus* PCC 7942 (C and D). A and C, Time courses of medium oxygen concentration (red traces) and relative Chl fluorescence (black traces). Initially, media containing cyanobacteria (10 μg Chl mL^{-1}) were kept dark; illumination with measuring light (ML) and actinic light (AL; 200 μmol photons m^{-2} s^{-1}) started as indicated. The downward shift in the Chl fluorescence signal (F_o) after the start of ML illumination is due to increasing the instrument amplification from 200 to 100 mV. Chl fluorescence parameters are as defined in the text. $NaHCO_3$ (final concentration, 10 mM) was added as indicated. α, β, and γ denote times at which oxygen evolution rates were determined in separate experiments. From about the time of maximum oxygen concentration to the addition of $NaHCO_3$, photosynthesis can be considered CO_2 limited. The experiments were performed four times, and representative data are shown. B and D, Time courses of Y(II), calculated for the corresponding measurements of F_m' as $(F_m' - F_s)/F_m'$. Values shown are means ± SD (n = 4).

photosynthetic CO_2 consumption and diffusion from the atmosphere), and γ (high CO_2 availability due to added $NaHCO_3$; compare Supplemental Fig. S1). In both strains, oxygen evolution rates were similarly high at times α and γ, indicating CO_2-saturated photosynthesis, and low at time β, indicating CO_2-limited photosynthesis (Table I). Under these conditions, the gradual drop of F_s and the parallel increase of Y(II) (Fig. 1, A and B) in *Synechocystis* sp. PCC 6803 strongly suggested the operation of an AEF under CO_2-limited photosynthesis.

F_m' increased during the transition (Fig. 1). The increase in F_m' could be caused by a state transition from state II to state I (McConnell et al., 2002). However, low-temperature fluorescence spectra of *Synechocystis* sp. PCC 6803 and *S. elongatus* PCC 7942 showed no changes during the transition to CO_2-limited photosynthesis (Miller et al., 1996; Hayashi et al., 2014). Thus, there is no evidence to support a state transition. The molecular mechanism for the increase in F_m' remains unknown. Therefore, we focused on the responses of AEF to the electron sink limitation that occurred during the shift from CO_2-saturated to CO_2-limited photosynthesis.

Synechocystis sp. PCC 6803, in which the transition from CO_2-saturated to CO_2-limited photosynthesis appeared to induce AEF, has four *flv* genes in its genome: *flv1* (*sll1521*), *flv2* (*sll0219*), *flv3* (*sll0550*), and *flv4* (*sll0217*). The activity of isozymes FLV2 and FLV4 seems to increase in response to low-[CO_2] conditions (Zhang et al., 2009; Eisenhut et al., 2012). A double mutant deficient in *flv1* and *flv3* showed the same response of Y(II) to the transition from CO_2-saturated to CO_2-limited photosynthesis as wild-type *Synechocystis* sp. PCC 6803 (Hayashi et al., 2014). Furthermore, the genes encoding FLV2 and FLV4 are absent from the genome of *S. elongatus* PCC 7942 (Bersanini et al., 2014), while *flv1* and *flv3* are present (*Synpcc7942_1810*, ortholog of *flv1*; *Synpcc7942_1809*, ortholog of *flv3*). We hypothesized that FLV2 and FLV4 are involved in the AEF under CO_2-limited photosynthesis and constructed mutants deficient in *flv2* and *flv4* (*Δflv2* and *Δflv4*, respectively; Supplemental Figs. S2 and S3). In contrast to the double mutant deficient in *flv1/3* (Hayashi et al., 2014), neither *Δflv2* nor *Δflv4* showed any increase in Y(II) during the transition from CO_2-saturated to CO_2-limited photosynthesis (Fig. 2, B and D), while F_s increased and then maintained its level (Fig. 2, A and C). On addition of $NaHCO_3$, F_s decreased and Y(II) recovered to values found under CO_2-saturated photosynthesis. The oxygen evolution rates in *Δflv2* and *Δflv4* decreased from time α to time β and recovered at time γ (Table I). Thus, suppression of Y(II) in *Δflv2* and *Δflv4* was due to the limited capacity of the CO_2-dependent electron sink, which could not be substituted by AEF. We concluded that in *Synechocystis* sp. PCC 6803, FLV2 and FLV4 are necessary for AEF under CO_2-limited photosynthesis. FLV2 and FLV4 form heterodimers (Zhang et al., 2012), and deletion of *flv4* suppresses the production of FLV2 (Eisenhut et al., 2012). Thus, deficiency in either of the two genes resulted in the complete loss of physiological function (Fig. 2).

The GST-FLV4 Fusion Protein Reduces Oxygen to Water

In *Synechocystis* sp. PCC 6803, FLV2 and FLV4 are required for AEF under CO_2-limited photosynthesis (Fig. 2), which also depends on the presence of oxygen in the *flv1/3* double mutant (Hayashi et al., 2014). These facts suggested that FLV2 and FLV4 donate electrons to oxygen. To determine whether oxygen can accept electrons from FLV2 and FLV4 in vitro, we expressed recombinant GST-FLV2 and GST-FLV4 fusion proteins in *Escherichia coli* and tried to purify them by affinity chromatography (Supplemental Fig. S4). Unfortunately, GST-FLV2 could not be separated from a contaminant protein of about 60 to 65 kD (Supplemental Fig. S4). Therefore, we could only examine the GST-FLV4 protein in the following experiments.

GST-FLV4 catalyzed the oxidation of NADH as monitored by the decrease in A_{340}. The K_m value for NADH was approximately 30 μM (Supplemental Fig. S5), similar to that of the recombinant FLV3 protein (Vicente et al., 2002). We could not obtain K_m for the NADPH-dependent oxygen reduction, owing to the significantly lower activity. GST-FLV4 also reduced oxygen using NADH as the electron donor (Fig. 3). Addition of GST-FLV4 to a reaction mixture containing 50 mM Tris-HCl (pH 7.4) and 1 mM NADH stimulated the reduction of oxygen at the rate of 20.2 ± 1.5 min^{-1} (Fig. 3). No oxygen depletion was observed when GST protein was added to the reaction mixture as a control. When catalase was added, no oxygen evolved, indicating that GST-FLV4 reduces oxygen to water without generating reactive

Table I. *Oxygen-exchange rates (μmol oxygen mg^{-1} Chl h^{-1}) in the dark, under CO_2-saturated and CO_2-limited photosynthesis, and after the addition of $NaHCO_3$ in Synechocystis sp. PCC 6803, S. elongatus PCC 7942, and the Δflv2 and Δflv4 mutants of Synechocystis sp. PCC 6803*

Oxygen-exchange rates were determined simultaneously with Chl fluorescence measurements under actinic light (200 μmol photons m^{-2} s^{-1}) at the times marked as α, β, and γ in Figure 1 and Supplemental Figure S1. The reaction mixture contained cyanobacterial cells (10 μg Chl mL^{-1}) and 50 mM HEPES-KOH (pH 7.5). Oxygen-exchange rates in the dark were determined before illuminating with measuring light. Negative values indicate oxygen uptake. Values are means ± SD of four independent experiments.

Condition	*Synechocystis* sp. PCC 6803	*S. elongatus* PCC 7942	*Δflv2*	*Δflv4*
Dark	−12.6 ± 2.1	−16 ± 4	−11 ± 5	−11 ± 3
CO_2-saturated photosynthesis (α)	129 ± 8	90 ± 15	129 ± 9	129 ± 24
CO_2-limited photosynthesis (β)	8 ± 5	3.6 ± 0.6	6 ± 4	7 ± 5
Addition of $NaHCO_3$ (γ)	114 ± 11	68 ± 10	108 ± 15	111 ± 10

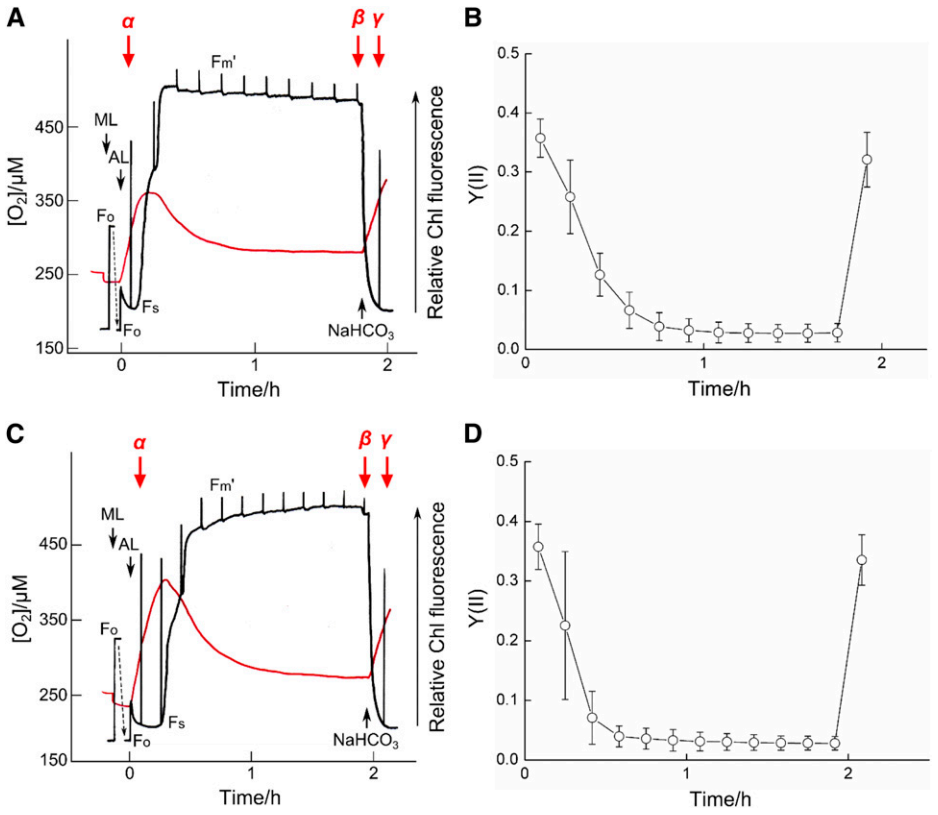

Figure 2. Development of photosynthetic parameters in media containing two high-[CO_2]-grown mutants of *Synechocystis* sp. PCC 6803, *Δflv2* (A and B) and *Δflv4* (C and D). All further details are as given in Figure 1.

oxygen species (Fig. 3). Furthermore, addition of dithionite showed that oxygen was completely consumed (Fig. 3). The K_m value for oxygen was below 10 μM. These results demonstrate the oxygen-reducing activity of GST-FLV4, which resembles that of the recombinant FLV3 protein (Vicente et al., 2002).

Photorespiration Does Not Contribute to Y(II) under CO_2-Limited Photosynthesis

In general, the oxygenation of ribulose-1,5-bisphosphate by Rubisco is presumed to be suppressed in cyanobacteria, because CCM maintains [CO_2] high around Rubisco in the carboxysome (Badger and Price, 1992), but *Synechocystis* sp. PCC 6803 may be an exception (Eisenhut et al., 2006, 2008). Cyanobacterial photorespiration may operate through three routes, the canonical plant-like C2 cycle and two cyanobacteria-specific routes, the glycerate and decarboxylation pathways (Hagemann et al., 2013). Allahverdiyeva et al. (2011) demonstrated photorespiratory oxygen uptake in the *flv1/3* double mutant by membrane inlet mass spectrometry. This opened the possibility that not only FLV2/4 but also photorespiration could be responsible for the increase in Y(II) under CO_2-limited photosynthesis in *Synechocystis* sp. PCC 6803 (Fig. 1). We constructed the mutants *Δpgp*, *ΔglcD1/2*, *ΔgcvT*, and *Δglyk*, which were deficient in the genes encoding phosphoglycolate phosphatase (*slr0458*), glycolate dehydrogenase (*sll0404* and *slr0806*), Gly decarboxylase T-protein (*sll0171*), and glycerate kinase (*slr1840*), respectively. These genes supposedly function in the canonical C2 cycle (Eisenhut et al., 2008). Inactivation of these genes in the mutants was confirmed by PCR analysis (Supplemental Figs. S2 and S3). All mutants showed the same Y(II) increase following the transition from CO_2-saturated to CO_2-limited photosynthesis as the wild-type *Synechocystis* sp. PCC 6803 (Supplemental Fig. S6; Supplemental Table S1), indicating that the C2 cycle was not involved in the Y(II) response.

DISCUSSION

We aimed at elucidating the molecular mechanism of AEF under CO_2-limited photosynthesis in *Synechocystis* sp. PCC 6803, reported in our previous study (Hayashi et al., 2014). On the transition from CO_2-saturated to CO_2-limited photosynthesis, LEF was transiently suppressed but then recovered to a value corresponding to the photosynthetic electron flux observed under CO_2-saturated photosynthesis. This implied the induction of AEF under CO_2-limited photosynthesis. We hypothesized that among the four FLV proteins in *Synechocystis* sp. PCC 6803, FLV2 and FLV4 could be involved because, first, the *flv1/3* double mutant showed the same response as the wild type (Hayashi et al., 2014), and second, FLV2 and FLV4 were produced under low-[CO_2] conditions (Zhang et al., 2009; Eisenhut et al., 2012). We confirmed that

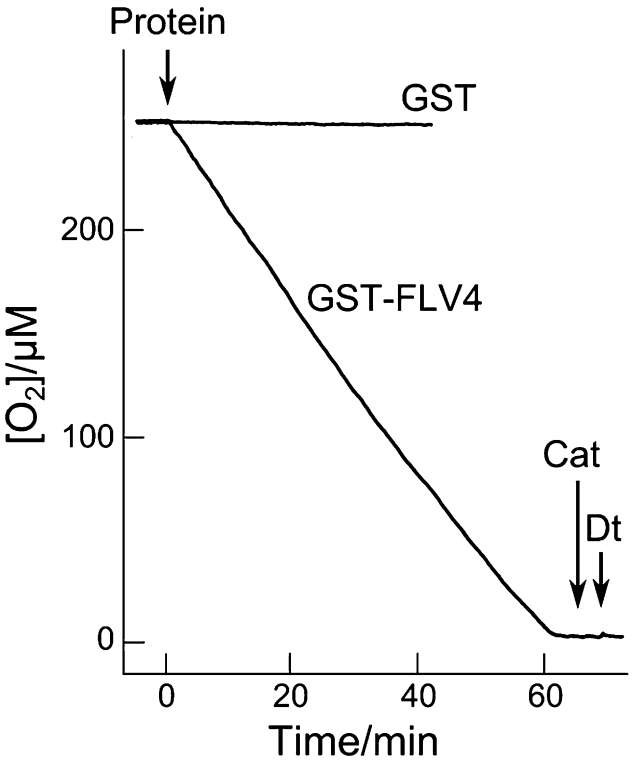

Figure 3. Oxygen-reducing activities of recombinant GST and GST-FLV4 fusion protein. The reaction mixture contained 50 mM Tris-HCl (pH 7.4), 1 mM NADH, and the protein of interest (40 μg). Catalase (Cat; 200 units mL^{-1}) and dithionite (Dt; 1 mM) were added as indicated. Purified GST protein served as a control.

Synechocystis sp. PCC 6803 mutants deficient in FLV2 and FLV4 cannot maintain LEF during the transition to CO_2-limited photosynthesis (Fig. 2), implying that FLV2 and FLV4 function in the AEF under CO_2-limited photosynthesis. In summary (Fig. 4), we propose that under CO_2-saturated photosynthesis, FLV1 and FLV3 operate (Helman et al., 2003; Allahverdiyeva et al., 2013; Hayashi et al., 2014) while FLV2 and FLV4 do not, whereas under CO_2-limited photosynthesis, FLV2 and FLV4 operate in addition to FLV1 and FLV3 to mediate AEF, thus contributing to the alleviation of photooxidative stress (Zhang et al., 2009, 2012).

The most striking finding is that FLV2 and FLV4 together have the capacity to replace the steady-state photosynthetic electron flux observed under CO_2-saturated photosynthesis (Figs. 1 and 2) by an AEF under CO_2-limited conditions. In wild-type *Synechocystis* sp. PCC 6803 performing CO_2-limited photosynthesis, Y(II) remained at 80% to 90% of that at CO_2-saturated photosynthesis (Fig. 1). In *Δflv2* and *Δflv4* under CO_2-limited conditions, Y(II) was only 5% to 10% of that at CO_2-saturated photosynthesis, corresponding to the extent of the concomitant reduction of photosynthetic oxygen evolution (Fig. 2; Table I). These findings suggest that FLV2 and FLV4 are sufficient to maintain AEF activity under low $[CO_2]$.

Under CO_2-depleted conditions, photorespiratory oxygen uptake in *Δflv1/3* occurred at rates (about 50 μmol oxygen mg^{-1} Chl h^{-1}) that exceeded the oxygen-photoreducing rate of FLV1/3 (approximately 30 μmol oxygen mg^{-1} Chl h^{-1}; Allahverdiyeva et al., 2011), indicating that photorespiration can function as an electron sink under CO_2-depleted as well as FLV1/3-depleted conditions (Helman et al., 2003; Allahverdiyeva et al., 2011). Unfortunately, we were unable to obtain evidence

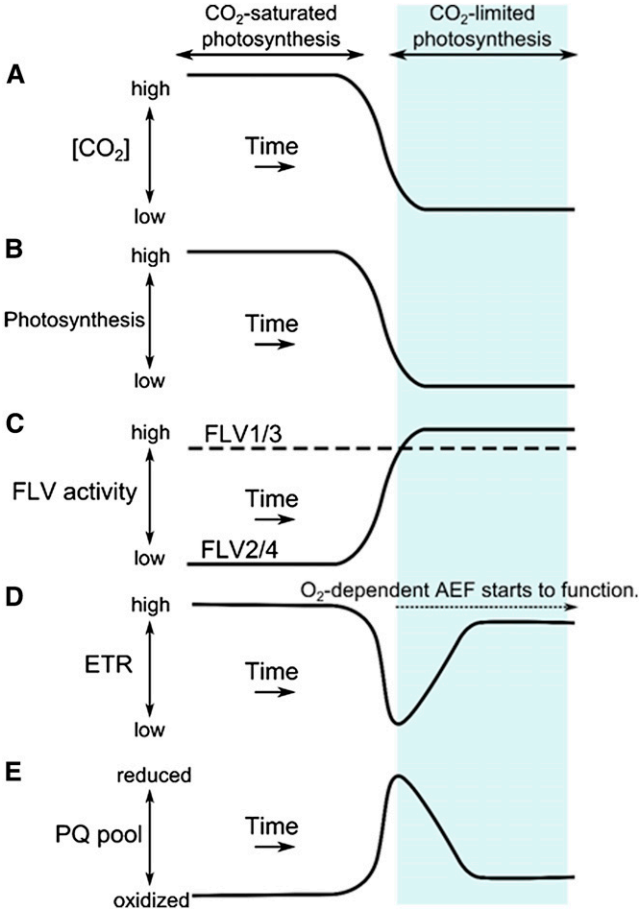

Figure 4. Model of the responses of photosynthesis, FLV activity, electron transport rate (ETR), and oxidation state of the PQ pool to the shift from CO_2-saturated to CO_2-limited photosynthesis in *Synechocystis* sp. PCC 6803. This model presents an interpretation of the processes occurring in the experiment shown in Figure 1A. A, CO_2 depletion by photosynthesis. Medium $[CO_2]$ decreases due to photosynthetic consumption following the start of illumination. B, Suppression of photosynthesis by photosynthesis-induced CO_2 depletion. Photosynthetic CO_2 consumption cannot be balanced by the diffusion of atmospheric CO_2 into the medium. C, Activities of FLV proteins. FLV1 and FLV3 function under CO_2-saturated and CO_2-limited conditions, while FLV2 and FLV4 become functional as mediators of AEF only under CO_2-limited conditions. D, Total ETR under CO_2-saturated photosynthesis is driven mainly by photosynthesis. A similar rate is maintained under CO_2 limitation by an oxygen-dependent AEF. E, Changes in the redox state of the PQ pool. Under CO_2-limited photosynthesis, the oxidized state is preserved by the FLV2/4-mediated, oxygen-dependent AEF.

in support of this idea (Supplemental Fig. S6). On the other hand, our data are in agreement with the interpretation that photorespiration operates in wild-type cells. For example, *ΔglcD1/2* and *ΔgcvT* mutants showed retarded growth (data not shown), as reported by Eisenhut et al. (2006, 2008). In addition, the initial F_m' was lower in *ΔglcD1/2* than in other strains (Supplemental Fig. S6), possibly owing to phycobilisome functions including state transition. A physiological role for cyanobacterial photorespiration has been proposed by Eisenhut et al. (2006, 2008), who reported that in *Synechocystis* sp. PCC 6803, photorespiration is not an electron sink but rather a scavenging system for toxic intermediates, notably glyoxylate (Eisenhut et al., 2008).

Supposedly, the electron acceptor for FLV2 and FLV4 is oxygen. Hayashi et al. (2014) reported that AEF activity under CO_2-limited photosynthesis in *Synechocystis* sp. PCC 6803 cells requires oxygen. We showed that AEF requires FLV2 and FLV4 (Fig. 2) and that the GST-FLV4 fusion protein possesses oxygen-reducing activity (Fig. 3), similar to recombinant FLV3 (Vicente et al., 2002). These results suggest that FLV2 and FLV4 use oxygen as an electron acceptor in vivo and in vitro. In contrast, FLV2 and FLV4 interact with PSII and phycobilisomes (Zhang et al., 2012; Bersanini et al., 2014). Therefore, FLV2 and FLV4 may catalyze the photoreduction of oxygen to water associated with PSII under CO_2-limited conditions in *Synechocystis* sp. PCC 6803. We did not succeed in preparing stable FLV2/4 heterodimers (data not shown). The molecular mechanism of FLV2/4 heterodimer function at PSII awaits its biochemical characterization in the future.

Under low-[CO_2] conditions, *Δflv2* and *Δflv4* showed severe photoinhibition of PSII (Zhang et al., 2009, 2012). Moreover, an overexpression mutant of the *flv4-2* operon in *Synechocystis* sp. PCC 6803 exhibited a more oxidized state of the PQ pool and a reduced production of singlet oxygen and showed resistance to photoinhibition of PSII (Bersanini et al., 2014). In wild-type *Synechocystis* sp. PCC 6803 under CO_2-limited photosynthesis, Y(II) remained high (Figs. 1 and 2; Hayashi et al., 2014), a property expected to contribute to the survival of *Synechocystis* sp. PCC 6803 in nature, where CO_2 assimilation would proceed under the CO_2-limited photosynthesis condition.

We attribute the low capacity for AEF in *S. elongatus* PCC 7942 to the loss of FLV2 and FLV4. *S. elongatus* PCC 7942 and *Synechocystis* sp. PCC 6803 are β-type cyanobacteria, but in contrast to *Synechocystis* sp. PCC 6803, *S. elongatus* PCC 7942 does not harbor the gene for the orange carotenoid protein responsible for the nonphotochemical quenching of Chl fluorescence (Boulay et al., 2008). *Synechocystis* sp. PCC 6803 mutants deficient in orange carotenoid protein suffer from photoinhibition under low-[CO_2] and high-light stress conditions (Wilson et al., 2006). The *Synechocystis* sp. PCC 6803 mutant deficient in FLV2/4 showed photoinhibition and growth inhibition under these conditions (Zhang et al., 2009, 2012). This suggests that *S. elongatus* PCC 7942 should lack tolerance against electron sink limitations such as those occurring under high light and low [CO_2], in contrast to *Synechocystis* sp. PCC 6803. However, Bersanini et al. (2014) proposed that in cyanobacteria such as *S. elongatus* PCC 7942 that lack FLV2 and FLV4, photoinhibition is alleviated by the expression of an additional copy of the reaction center protein in PSII, D1, called D1:2, which enhances the tolerance against photo stress (Clarke et al., 1993). The relationship between this photoprotective system and FLV2/4 calls for further study.

Since the report of Asada and Badger (1984), the oxygen-dependent AEF (Mehler reaction in chloroplasts) has been quantitatively investigated in various photosynthetic organisms. In intact chloroplasts of higher plants, oxygen-dependent AEF amounted to 10% to 20% of the photosynthetic electron flux coupled to CO_2 fixation (Badger et al., 2000). The proportion is as low as 1% to 10% according to a recent study, which would seem to suggest that the Mehler reaction is not a major electron sink in higher plants (Driever and Baker, 2011). In intact leaves of C_3 plants, photorespiration could be a major electron sink under conditions of CO_2-limited photosynthesis (Driever and Baker, 2011; Shirao et al., 2013). These conclusions cannot necessarily be extended to cyanobacteria and algae, which seem to have higher Mehler reaction activities than higher plants (Badger et al., 2000). In fact, the diatom *Thalassiosira pseudonana* showed oxygen photoreduction at a rate of 600 μmol mg^{-1} Chl h^{-1}, corresponding to 49% of the electron flux through PSII (Waring et al., 2010). Similarly, the oxygen-dependent electron transport rate contributes 30% of the total electron flux in *Symbiodinium* sp., a group of symbiotic dinoflagellates of cnidarians, and FLV proteins might be involved (Roberty et al., 2014). In view of these reports and this study, algae and cyanobacteria appear to utilize oxygen-dependent AEFs other than photorespiration as major alternative electron sinks. Linking the physiological function of oxygen-dependent AEFs with their diversity among photosynthetic organisms is a fascinating topic for future investigations.

MATERIALS AND METHODS

Growth Conditions and Determination of Chl *a*

Synechocystis sp. PCC 6803 and *Synechococcus elongatus* PCC 7942 cells were cultured in BG-11 medium on a rotary shaker (100 rpm) under light/dark conditions (25°C, 16 h, 100 μmol photons m^{-2} s^{-1}, fluorescent lamp/23°C, 8 h, dark) in 2% (v/v) CO_2. For Chl quantification, cells were harvested and resuspended by vortexing in 1 mL of 100% (w/v) methanol. After incubation at room temperature for 5 min, the suspension was centrifuged at 10,000*g* for 5 min at room temperature. Chl *a* was determined by the method of Lee et al. (1998).

Generation of Mutants

To disrupt a gene (*pgp*, *slr0458*; *glcD1*, *sll0404*; *glcD2*, *slr0806*; *gcvT*, *sll0171*; *glyk*, *slr1840*; *flv2*, *sll0219*; and *flv4*, *sll0217*), the coding region was replaced with a cassette of the kanamycin resistance gene (*Kan^r*) or the chloramphenicol resistance gene (*Cm^r*) amplified from the pUC4-KIXX or pACYC184 vector, respectively (Nakahara et al., 2003), by PCR using appropriate f and r primer sets (listed in Supplemental Table S2). We constructed these mutants following

the method of Sakurai et al. (2007). The regions upstream and downstream of each gene were amplified by PCR using two sets of primers: up f and up r, and dn f and dn r, respectively. The front ends of up r and dn f contained regions that complemented the sequences of the primers *Kan*^{r} f and *Kan*^{r} r or *Cm*^{r} f and *Cm*^{r} r (Supplemental Table S2). We used three fragments, up, *Kan*^{r} or *Cm*^{r}, and dn, which were then linked by successive PCRs to obtain a disruption cassette. Sato et al. (2005) generated 40 mutants of *Synechocystis* sp. PCC 6803 by this high-throughput method.

Transformation of *Synechocystis* sp. PCC 6803 was performed by the standard procedure (Williams, 1988). Transformants were selected on 0.5% (w/v) agar plates of BG-11 medium containing 20 μg mL^{-1} kanamycin or 30 μg mL^{-1} chloramphenicol. The double mutant Δ*glcD1/2* was generated by transformation of the Δ*glcD2* (*slr0806*) mutant with the mutated Δ*glcD1* (*sll0404*). The resultant transformant was selected on 0.5% (w/v) agar plates of BG-11 medium containing 20 μg mL^{-1} kanamycin and 30 μg mL^{-1} chloramphenicol.

Measurement of Oxygen Concentration

The uptake and evolution of oxygen were measured simultaneously with Chl fluorescence. The reaction mixture (2 mL) containing 50 mM HEPES-KOH (pH 7.5) and cyanobacterial cells (10 μg Chl mL^{-1}) was illuminated with actinic light (red light, greater than 620 nm; 200 μmol photons m^{-2} s^{-1}) at 25°C. During the measurements, the reaction mixture was stirred with a magnetic microstirrer. In one set of experiments, oxygen concentrations were monitored continuously with an oxygen electrode while the measuring cuvette remained open to allow the diffusion of oxygen and CO_2 between the medium and the atmosphere (Hansatech; Hayashi et al., 2014). Typical results of this type of experiment are shown in Figures 1 and 2. In a second set of experiments, the top of the cuvette was temporarily (1–3 min) closed to determine the oxygen evolution rate. Typical data for the determination of oxygen evolution rate are shown in Supplemental Figure S1.

Measurement of Chl Fluorescence

The relative Chl fluorescence originating from Chl *a* was measured using a PAM-Chl fluorometer (PAM-101; Walz; Hayashi et al., 2014). Pulse-modulated excitation was achieved by a light-emitting diode lamp with peak emission at 650 nm. Modulated fluorescence was measured at the wavelength (>710 nm; Schott RG9 long-pass filter). The minimum Chl fluorescence was determined by illumination with measuring light. The F_s was monitored under actinic red light, and 1,000-ms pulses of saturated light (10,000 μmol photons m^{-2} s^{-1}) were supplied at arbitrary intervals to determine the F_m'. Y(II) was defined as $(F_m' - F_s)/F_m'$. The fluorescence terminology used in this study follows van Kooten and Snel (1990).

Cloning and Expression of Recombinant GST-FLV2/4 Fusion Proteins

The coding regions of FLV2 and FLV4 were obtained from the genomic DNA of *Synechocystis* sp. PCC 6803 using KOD-FX Neo (Toyobo) and subcloned via *Bam*HI into pGEX4T-3 (GE Healthcare) using the In-Fusion HD cloning kit (Takara). The primers for these genes are listed in Supplemental Table S3. Recombinant proteins were produced in BL21 (Agilent Technology) host cells. Overnight cultures of the transformed BL21 cells in Luria-Bertani broth were used to inoculate (0.1% [v/v]) fresh Luria-Bertani broth, which was then incubated at 37°C until the A_{600} reached 0.5 to 1. Protein expression was evaluated at 15°C for 16 h in Luria-Bertani broth containing 0.1 mM isopropyl-β-D-thiogalactopyranoside.

Purification of Recombinant GST Fusion Proteins

Cells were harvested by centrifugation and resuspended in phosphate-buffered saline buffer (140 mM NaCl, 2.7 mM KCl, 10 mM Na_2HPO_4, 1.8 mM KH_2PO_4, and 1 mM phenylmethylsulfonyl fluoride [pH 7.3]). After gentle sonication, the resulting crude extract was centrifuged at 15,000 rpm for 30 min at 4°C. The lysate was loaded onto GSTrap FF columns (GE Healthcare). Unbound proteins were removed by washing with phosphate-buffered saline buffer. Recombinant GST fusion proteins were then eluted with elution buffer (50 mM Tris-HCl, 10 mM reduced glutathione, and 1 mM phenylmethylsulfonyl fluoride [pH 8]). The purified recombinant protein was quantified using the Pierce 660-nm protein assay (Thermo Scientific). Fractions containing 0.1 μg of purified recombinant proteins were analyzed by SDS-PAGE and stained with Coomassie Brilliant Blue to evaluate the purity of the recombinant proteins (Supplemental Fig. S4). After electrophoresis, the proteins were electrotransferred to a polyvinylidene fluoride membrane and detected by GST-specific antibodies (Novagen; Supplemental Fig. S4). We used the purified GST protein as a control. The GST protein was expressed in BL21 containing a blank pGEX4T-3 vector.

Enzyme Assays

The NADH-oxidizing activity of recombinant GST-FLV4 fusion protein was evaluated in a reaction mixture (1 mL) containing 50 mM Tris-HCl (pH 7.4), 10 μg of GST-FLV4 protein, and various concentrations of NADH. The FLV-dependent oxidation of NADH was monitored as the decrease in A_{340} at 25°C, assuming an absorption coefficient of 6.22 mM cm^{-1}.

The oxygen-reducing activities of the recombinant GST and GST-FLV4 proteins were evaluated in a reaction mixture (2 mL) containing 50 mM Tris-HCl (pH 7.4), 1 mM NADH, and the protein of interest (40 μg). GST protein was used as the control. GST- and GST-FLV-dependent oxygen reductions were measured with an oxygen electrode (Hansatech).

Supplemental Data

The following supplemental materials are available.

Supplemental Figure S1. Determination of oxygen evolution rates during the development of photosynthetic parameters in the *Synechocystis* sp. PCC 6803 wild type.

Supplemental Figure S2. Maps of the insertion sites of antibiotic resistance cassettes in Δ*pgp*, Δ*glcD1/2*, Δ*gcvT*, Δ*glyk*, Δ*flv2*, and Δ*flv4*.

Supplemental Figure S3. DNA fragments amplified by PCR showing complete segregation of the inactivated genes *pgp* (*slr0458*), *glcD1* (*sll0404*), *glcD2* (*slr0806*), *gcvT* (*sll0171*), *glyk* (*slr1840*), *flv2* (*sll0219*), and *flv4* (*sll0217*).

Supplemental Figure S4. SDS-PAGE and western blot of GST, GST-FLV2, and GST-FLV4 proteins.

Supplemental Figure S5. Dependence of the NADH oxidation activity on the concentration of NADH in the reaction catalyzed by the recombinant GST-FLV4 protein.

Supplemental Figure S6. Development of photosynthetic parameters in media containing high-[CO_2]-grown Δ*pgp*, Δ*glcD1/2*, Δ*gcvT*, and Δ*glyk* mutants of *Synechocystis* sp. PCC 6803.

Supplemental Table S1. Oxygen-exchange rates in the dark, under CO_2-saturated and CO_2-limited photosynthesis, and after the addition of $NaHCO_3$, in four mutants of *Synechocystis* sp. PCC 6803 (Δ*pgp*, Δ*glcD1/2*, Δ*gcvT*, and Δ*glyk*).

Supplemental Table S2. Oligonucleotides used for the disruption of the *pgp*, *glcD1/2*, *gcvT*, *glyk*, *flv2*, and *flv4* genes.

Supplemental Table S3. Oligonucleotides used for the construction of FLV2 and FLV4 expression vectors.

ACKNOWLEDGMENTS

We thank NAI, Inc. (http://www.nai.co.jp/) for the English language revision.

Received September 6, 2014; accepted December 23, 2014; published December 24, 2014.

LITERATURE CITED

Allahverdiyeva Y, Ermakova M, Eisenhut M, Zhang P, Richaud P, Hagemann M, Cournac L, Aro EM (2011) Interplay between flavodiiron proteins and photorespiration in *Synechocystis* sp. PCC 6803. J Biol Chem **286:** 24007–24014

Allahverdiyeva Y, Mustila H, Ermakova M, Bersanini L, Richaud P, Ajlani G, Battchikova N, Cournac L, Aro EM (2013) Flavodiiron proteins Flv1 and Flv3 enable cyanobacterial growth and photosynthesis under fluctuating light. Proc Natl Acad Sci USA **110:** 4111–4116

Appel J, Phunpruch S, Steinmüller K, Schulz R (2000) The bidirectional hydrogenase of *Synechocystis* sp. PCC 6803 works as an electron valve during photosynthesis. Arch Microbiol **173:** 333–338

Asada K, Badger MR (1984) Photoreduction of $^{18}O_2$ and $H_2{}^{18}O_2$ with concomitant evolution of $^{16}O_2$ in intact spinach chloroplasts: evidence for scavenging of hydrogen peroxide by peroxidase. Plant Cell Physiol **25:** 1169–1179

Badger MR, Price GD (1992) The CO_2 concentrating mechanism in cyanobacteria and microalgae. Physiol Plant **84:** 606–615

Badger MR, von Caemmerer S, Ruuska S, Nakano H (2000) Electron flow to oxygen in higher plants and algae: rates and control of direct photoreduction (Mehler reaction) and Rubisco oxygenase. Philos Trans R Soc Lond B Biol Sci **355:** 1433–1446

Berry S, Schneider D, Vermaas WFJ, Rögner M (2002) Electron transport routes in whole cells of Synechocystis sp. strain PCC 6803: the role of the cytochrome bd-type oxidase. Biochemistry **41:** 3422–3429

Bersanini L, Battchikova N, Jokel M, Rehman A, Vass I, Allahverdiyeva Y, Aro EM (2014) Flavodiiron protein Flv2/Flv4-related photoprotective mechanism dissipates excitation pressure of PSII in co-operation with phycobilisomes in cyanobacteria. Plant Physiol **164:** 805–818

Boulay C, Abasova L, Six C, Vass I, Kirilovsky D (2008) Occurrence and function of the orange carotenoid protein in photoprotective mechanisms in various cyanobacteria. Biochim Biophys Acta **1777:** 1344–1354

Clarke AK, Hurry VM, Gustafsson P, Oquist G (1993) Two functionally distinct forms of the photosystem II reaction-center protein D1 in the cyanobacterium *Synechococcus* sp. PCC 7942. Proc Natl Acad Sci USA **90:** 11985–11989

Driever SM, Baker NR (2011) The water-water cycle in leaves is not a major alternative electron sink for dissipation of excess excitation energy when CO_2 assimilation is restricted. Plant Cell Environ **34:** 837–846

Eisenhut M, Georg J, Klähn S, Sakurai I, Mustila H, Zhang P, Hess WR, Aro EM (2012) The antisense RNA As1_flv4 in the cyanobacterium *Synechocystis* sp. PCC 6803 prevents premature expression of the *flv4-2* operon upon shift in inorganic carbon supply. J Biol Chem **287:** 33153–33162

Eisenhut M, Kahlon S, Hasse D, Ewald R, Lieman-Hurwitz J, Ogawa T, Ruth W, Bauwe H, Kaplan A, Hagemann M (2006) The plant-like C2 glycolate cycle and the bacterial-like glycerate pathway cooperate in phosphoglycolate metabolism in cyanobacteria. Plant Physiol **142:** 333–342

Eisenhut M, Ruth W, Haimovich M, Bauwe H, Kaplan A, Hagemann M (2008) The photorespiratory glycolate metabolism is essential for cyanobacteria and might have been conveyed endosymbiontically to plants. Proc Natl Acad Sci USA **105:** 17199–17204

Flores E, Frías JE, Rubio LM, Herrero A (2005) Photosynthetic nitrate assimilation in cyanobacteria. Photosynth Res **83:** 117–133

Hagemann M, Fernie AR, Espie GS, Kern R, Eisenhut M, Reumann S, Bauwe H, Weber APM (2013) Evolution of the biochemistry of the photorespiratory C2 cycle. Plant Biol (Stuttg) **15:** 639–647

Hayashi R, Shimakawa G, Shaku K, Shimizu S, Akimoto S, Yamamoto H, Amako K, Sugimoto T, Tamoi M, Makino A, et al (2014) O_2-dependent large electron flow functioned as an electron sink, replacing the steady-state electron flux in photosynthesis in the cyanobacterium *Synechocystis* sp. PCC 6803, but not in the cyanobacterium *Synechococcus* sp. PCC 7942. Biosci Biotechnol Biochem **78:** 384–393

Helman Y, Tchernov D, Reinhold L, Shibata M, Ogawa T, Schwarz R, Ohad I, Kaplan A (2003) Genes encoding A-type flavoproteins are essential for photoreduction of O_2 in cyanobacteria. Curr Biol **13:** 230–235

Lea-Smith DJ, Ross N, Zori M, Bendall DS, Dennis JS, Scott SA, Smith AG, Howe CJ (2013) Thylakoid terminal oxidases are essential for the cyanobacterium *Synechocystis* sp. PCC 6803 to survive rapidly changing light intensities. Plant Physiol **162:** 484–495

Lee HM, Flores E, Herrero A, Houmard J, Tandeau de Marsac N (1998) A role for the signal transduction protein PII in the control of nitrate/nitrite uptake in a cyanobacterium. FEBS Lett **427:** 291–295

McConnell MD, Koop R, Vasil'ev S, Bruce D (2002) Regulation of the distribution of chlorophyll and phycobilin-absorbed excitation energy in cyanobacteria: a structure-based model for the light state transition. Plant Physiol **130:** 1201–1212

Miller AG, Espie GS, Bruce D (1996) Characterization of the non-photochemical quenching of chlorophyll fluorescence that occurs during the active accumulation of inorganic carbon in the cyanobacterium *Synechococcus* PCC 7942. Photosynth Res **49:** 251–262

Mullineaux CW (2014) Co-existence of photosynthetic and respiratory activities in cyanobacterial thylakoid membranes. Biochim Biophys Acta **1837:** 503–511

Nakahara K, Yamamoto H, Miyake C, Yokota A (2003) Purification and characterization of class-I and class-II fructose-1,6-bisphosphate aldolases from the cyanobacterium *Synechocystis* sp. PCC 6803. Plant Cell Physiol **44:** 326–333

Nomura CT, Persson S, Shen G, Inoue-Sakamoto K, Bryant DA (2006) Characterization of two cytochrome oxidase operons in the marine cyanobacterium *Synechococcus* sp. PCC 7002: inactivation of ctaDI affects the PS I:PS II ratio. Photosynth Res **87:** 215–228

Pils D, Schmetterer G (2001) Characterization of three bioenergetically active respiratory terminal oxidases in the cyanobacterium *Synechocystis* sp. strain PCC 6803. FEMS Microbiol Lett **203:** 217–222

Roberty S, Bailleul B, Berne N, Franck F, Cardol P (2014) PSI Mehler reaction is the main alternative photosynthetic electron pathway in *Symbiodinium* sp., symbiotic dinoflagellates of cnidarians. New Phytol **204:** 81–91

Sakurai I, Mizusawa N, Wada H, Sato N (2007) Digalactosyldiacylglycerol is required for stabilization of the oxygen-evolving complex in photosystem II. Plant Physiol **145:** 1361–1370

Sato N, Ishikawa M, Fujiwara M, Sonoike K (2005) Mass identification of chloroplast proteins of endosymbiont origin by phylogenetic profiling based on organism-optimized homologous protein groups. Genome Inform **16:** 56–68

Shirao M, Kuroki S, Kaneko K, Kinjo Y, Tsuyama M, Förster B, Takahashi S, Badger MR (2013) Gymnosperms have increased capacity for electron leakage to oxygen (Mehler and PTOX reactions) in photosynthesis compared with angiosperms. Plant Cell Physiol **54:** 1152–1163

van Kooten O, Snel JFH (1990) The use of chlorophyll fluorescence nomenclature in plant stress physiology. Photosynth Res **25:** 147–150

Vicente JB, Gomes CM, Wasserfallen A, Teixeira M (2002) Module fusion in an A-type flavoprotein from the cyanobacterium *Synechocystis* condenses a multiple-component pathway in a single polypeptide chain. Biochem Biophys Res Commun **294:** 82–87

Waring J, Klenell M, Bechtold U, Underwood GJC, Baker NR (2010) Light-induced responses of oxygen photoreduction, reactive oxygen species production and scavenging in two diatom species. J Phycol **46:** 1206–1217

Williams JGK (1988) Construction of specific mutations in photosystem II photosynthetic reaction center by genetic engineering methods in *Synechocystis* 6803. Methods Enzymol **167:** 766–778

Wilson A, Ajlani G, Verbavatz JM, Vass I, Kerfeld CA, Kirilovsky D (2006) A soluble carotenoid protein involved in phycobilisome-related energy dissipation in cyanobacteria. Plant Cell **18:** 992–1007

Zhang P, Allahverdiyeva Y, Eisenhut M, Aro EM (2009) Flavodiiron proteins in oxygenic photosynthetic organisms: photoprotection of photosystem II by Flv2 and Flv4 in *Synechocystis* sp. PCC 6803. PLoS ONE **4:** e5331

Zhang P, Eisenhut M, Brandt AM, Carmel D, Silén HM, Vass I, Allahverdiyeva Y, Salminen TA, Aro EM (2012) Operon *flv4-flv2* provides cyanobacterial photosystem II with flexibility of electron transfer. Plant Cell **24:** 1952–1971

Table S1. O_2 exchange rates in the dark, under CO_2-saturated and CO_2-limited photosynthesis, and after addition of $NaHCO_3$, in four mutants of *S.* 6803 (Δ*pgp*, Δ*glcD1/2*, Δ*gcvT*, and Δ*glyk*).

	Δ*pgp*	Δ*glcD1/2*	Δ*gcvT*	Δ*glyk*
Dark	–47 ± 19	–20 ± 6	–22 ± 12	–13 ± 4
CO_2-saturated photosynthesis (α)	110 ± 10	110 ± 17	122 ± 3	125 ± 16
CO_2-limited photosynthesis (β)	8.5 ± 2.3	5.9 ± 1.7	12 ± 7	8 ± 4
Addition of $NaHCO_3$ (γ)	98 ± 23	94 ± 8	98 ± 9	115 ± 7

O_2 exchange rates were determined simultaneously with Chl fluorescence measurement under actinic light (AL; 200 μmol photons m^{-2} s^{-1}) at the times indicated by α, β, and γ in Supplemental Fig. S6 (see also Fig. 1 and 2). The reaction mixture contained cyanobacterial cells (10 μg Chl mL^{-1}) and 50 mM HEPES-KOH (pH 7.5). The O_2 exchange rates in the dark were determined before illumination with measuring light (ML). Negative values indicate O_2 uptake. Values (μmol O_2 [mg Chl]$^{-1}$ h^{-1}) are means ± standard deviation, n = 4.

Table S2. Oligonucleotides used for the disruption of the *pgp*, *glcD1/2*, *gcvT*, *glyk*, *flv2*, and *flv4* genes.

Primer name	Sequence (5'-3')
Kan^r f	TAGACTGGGCGGTTTTATGG
Kan^r r	ATTCCGAAGCCCAACCTTT
Cm^r f	GATCGGCACGTAAGAGGTTC
Cm^r r	AGAAGCACACGGTCACACTG
slr0458 up f	GGAACCTACATTCGAGCCTTAGC
slr0458 up r	CCATAAAACCGCCCAGTCTAAGTTGGGGGAGATTTTCGATGTA
slr0458 dn f	AAAGGTTGGGCTTCGGAATATTACCGCATTCTAGCCTGCAC
slr0458 dn r	GGGAGACTGATGCAAAAACTCAC
sll0404 up f	GTGGCTACCTGTTCCGTTGT
sll0404 up r	GAACCTCTTACGTGCCGATCGAAGCTAATCCCAGCACCAA
sll0404 dn f	CAGTGTGACCGTGTGCTTCTCATCAGTTCTTGCCTGCTCA
sll0404 dn r	TGCCCAATATGTTCAACGAA
slr0806 up f	CTGGTTTGTCCCGCAATAAT
slr0806 up r	CCATAAAACCGCCCAGTCTAATTGCCTCTGGTTCTGATCG
slr0806 dn f	AAAGGTTGGGCTTCGGAATGTGATCGCCTGGAAGAAATC
slr0806 dn r	AATACACCTCCGGCAAACTG

Primer name	Sequence (5'-3')
sll0171 up f	ATTCTCTGAGCCGGAGAAATAGG
sll0171 up r	CCATAAAACCGCCCAGTCTACTGATCCACTAAAGGCTGCAAAA
sll0171 dn f	AAAGGTTGGGCTTCGGAATCAGAAGTGGGAAAACAACTCTGG
sll0171 dn r	CCCCTAAATCCCACTTAAAAAGG
slr1840 up f	TTTTGATTGCACCAGACTCTTTT
slr1840 up r	CCATAAAACCGCCCAGTCTAAACCCAATGCCATTAGTAAACCT
slr1840 dn f	AAAGGTTGGGCTTCGGAATTAGTACGGGAGTTTGATGGCTTT
slr1840 dn r	TGTTTCACTTGAACCAATCTTTT
sll0219 up f	CATTTCTGCTCATTCTGGGTGTT
sll0219 up r	CCATAAAACCGCCCAGTCTAGTAGGCAAGGTCATCAACTGGAG
sll0219 dn f	AAAGGTTGGGCTTCGGAATAATCTCGATGCCCTAGATGTTTG
sll0219 dn r	ACAGAAACACCGTTTTGCTCAGT
sll0217 up f	GCCATAGAGCCCTCTCGATAGAT
sll0217 up r	GAACCTCTTACGTGCCGATCGAAATCAGGTTCGAGTCGTTCTG
sll0217 dn f	CAGTGTGACCGTGTGCTTCTCAAGTTATCGGCCTGTTTGAAAG
sll0217 dn r	GAATCCACATTGGTTGAGAGGAG

All sequences are displayed in the 5′-to-3′ orientation.

Table S3. Oligonucleotides used for the construction of FLV2 and 4 expression vectors. All sequences are displayed in the 5′-to-3′ orientation.

Primer name	Sequence (5’-3’)
FLV2-Infusion f	GGTTCCGCGTGGATCCATGATTTCTCCAATTGGTGGTCTT
FLV2-Infusion r	GGGAATTCGGGGATCCTAATATTGTCCCCCCG
FLV4-Infusion f	GGTTCCGCGTGGATCCATGGTTACCCTAATTGATTCT
FLV4-Infusion r	GGGAATTCGGGGATCTTAGTAGTGGTTGCCCAGTTT

All sequences are displayed in 5’-3’ orientation.

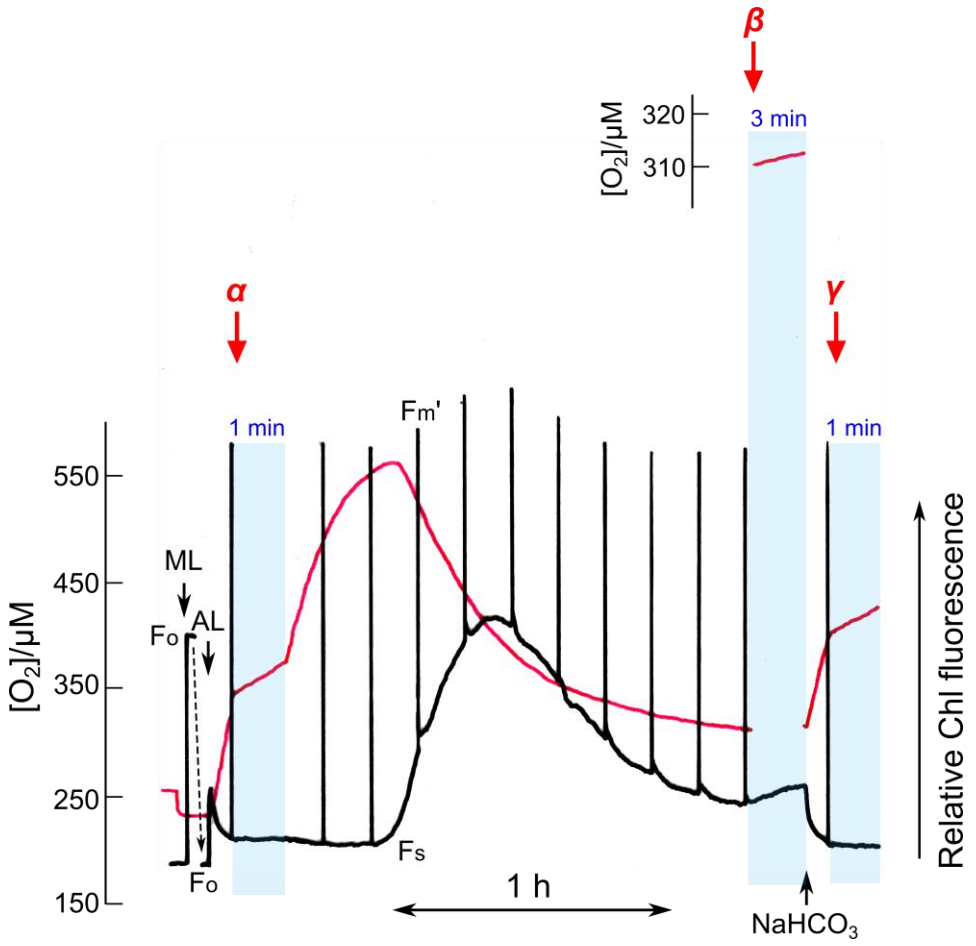

Fig. S1. Determination of O_2 evolution rates during the monitoring of medium [O_2] (red trace) and relative Chl fluorescence (black trace) in the *S.* 6803 wild type. A representative experiment is shown. At times *α*, *β*, and *γ*, the top of the O_2 electrode chamber was closed for 1−3 min (indicated by blue shading), and the O_2 evolution rates were determined. Thereafter, the chamber was opened again. For the measurement of the rate at *β*, the sensitivity of the recording was increased temporarily from 2 V to 500 mV. The medium containing *S.* 6803 cells (10 μg Chl mL^{-1}) was illuminated with actinic light (200 μmol photons m^{-2} s^{-1}) from the indicated starting time (AL). The cells were added to the medium before illumination with measuring light commenced (ML). Further details as in Fig. 1.

Figure S1. Shimakawa *et al.* (2014)

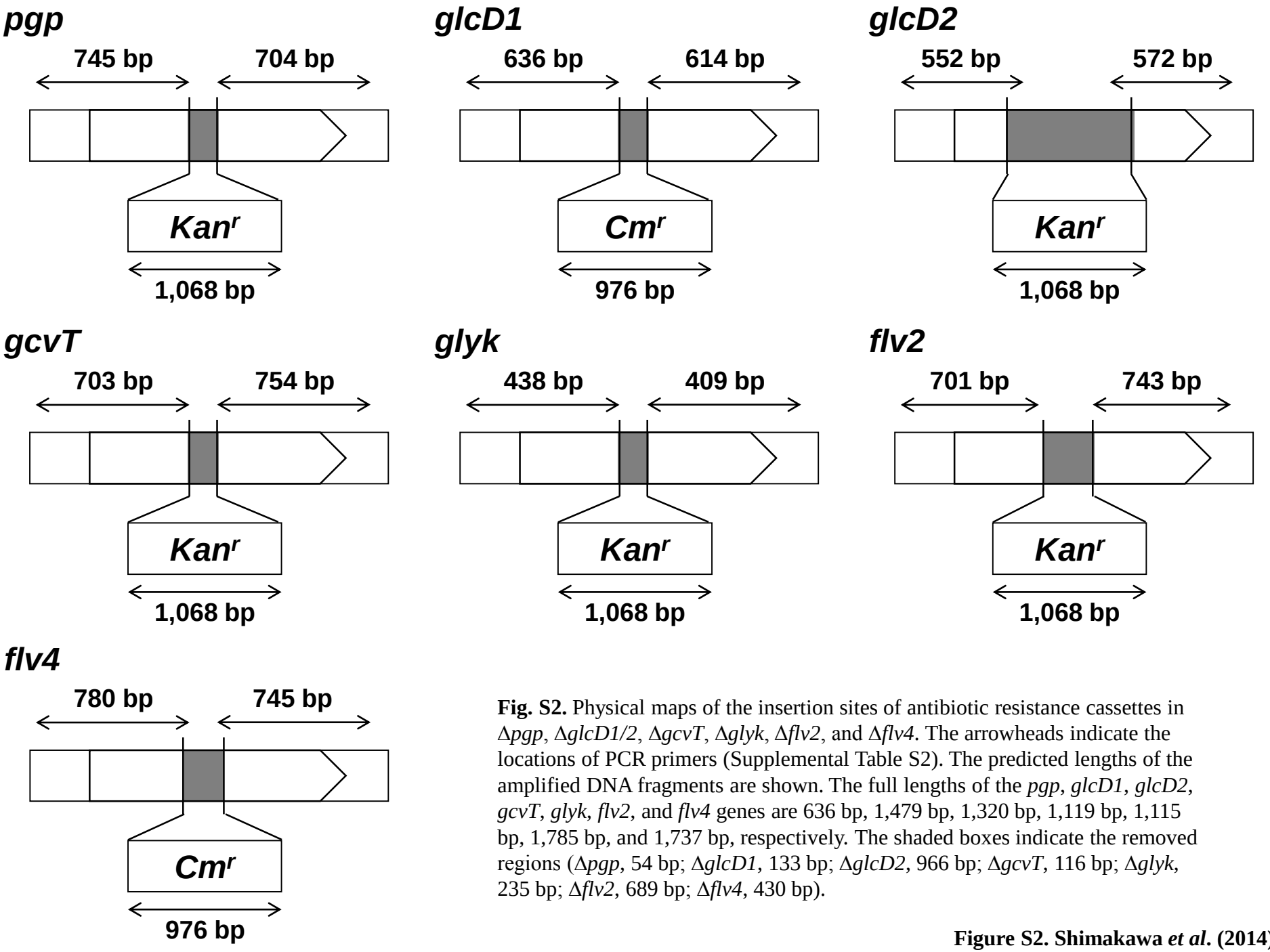

Fig. S2. Physical maps of the insertion sites of antibiotic resistance cassettes in Δ*pgp*, Δ*glcD1/2*, Δ*gcvT*, Δ*glyk*, Δ*flv2*, and Δ*flv4*. The arrowheads indicate the locations of PCR primers (Supplemental Table S2). The predicted lengths of the amplified DNA fragments are shown. The full lengths of the *pgp*, *glcD1*, *glcD2*, *gcvT*, *glyk*, *flv2*, and *flv4* genes are 636 bp, 1,479 bp, 1,320 bp, 1,119 bp, 1,115 bp, 1,785 bp, and 1,737 bp, respectively. The shaded boxes indicate the removed regions (Δ*pgp*, 54 bp; Δ*glcD1*, 133 bp; Δ*glcD2*, 966 bp; Δ*gcvT*, 116 bp; Δ*glyk*, 235 bp; Δ*flv2*, 689 bp; Δ*flv4*, 430 bp).

Figure S2. Shimakawa *et al*. (2014)

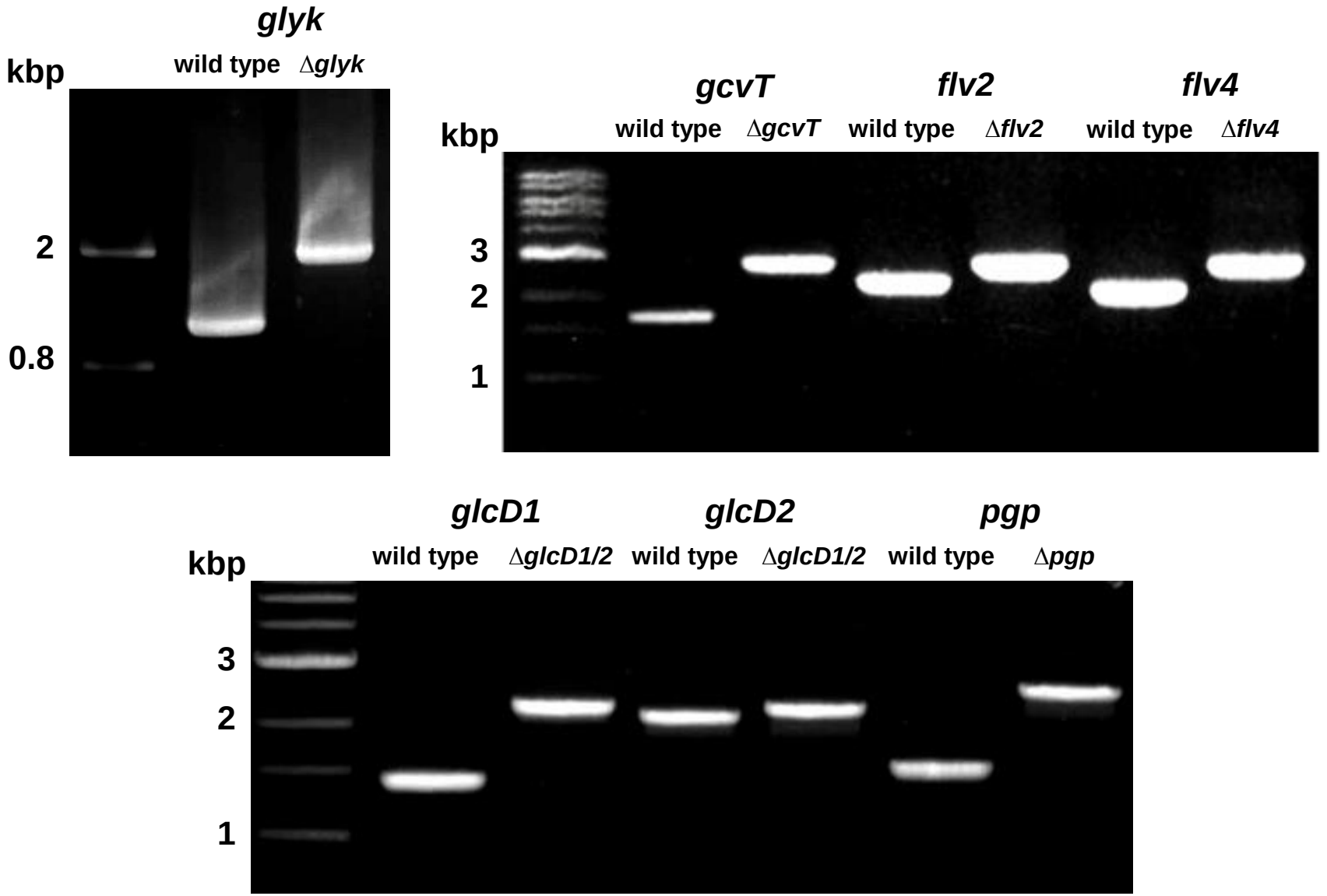

Fig. S3. DNA fragments amplified by PCR showing complete segregation of the inactivated genes, *pgp* (*slr0458*), *glcD1* (*sll0404*), *glcD2* (*slr0806*), *gcvT* (*sll0171*), *glyk* (*slr1840*), *flv2* (*sll0219*), and *flv4* (*sll0217*).

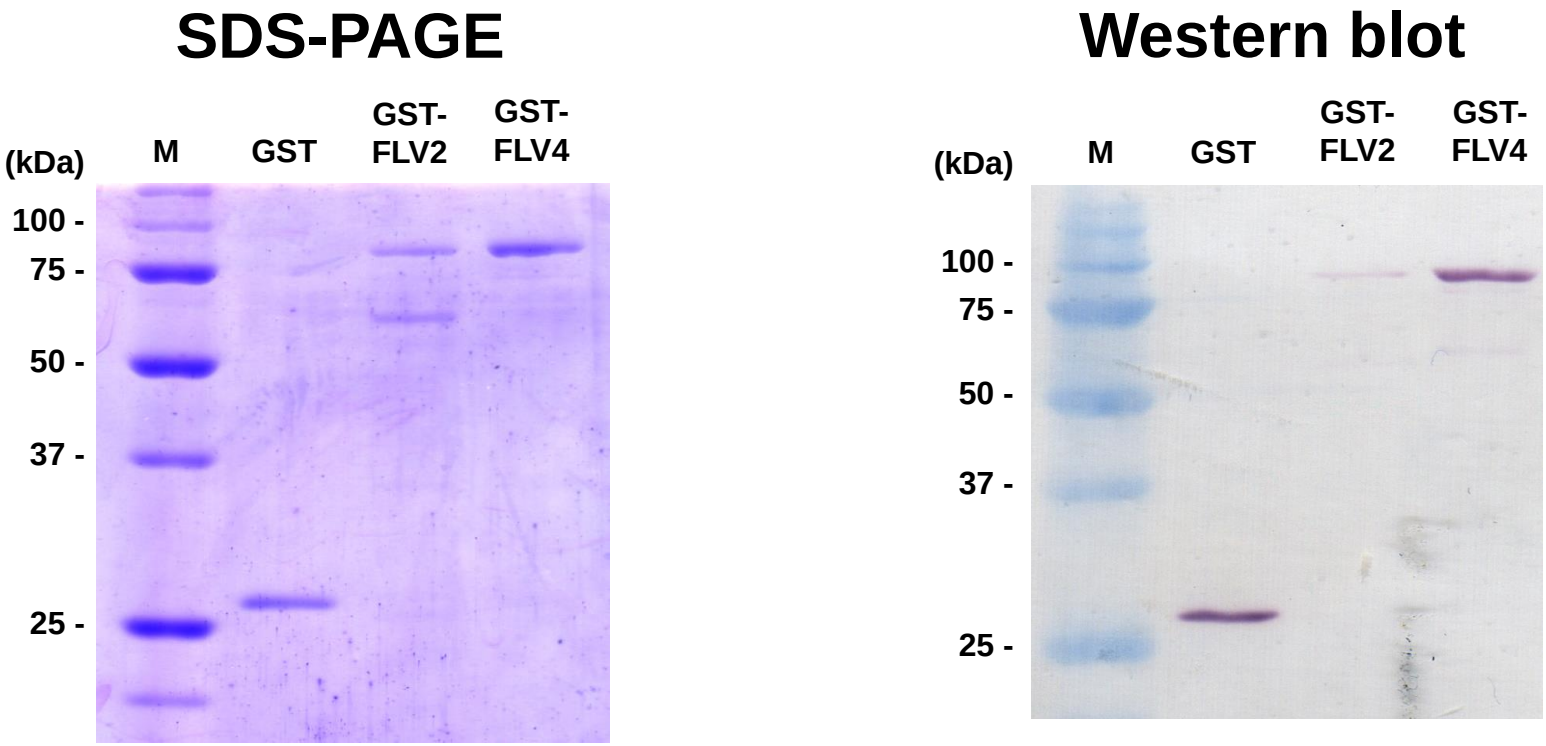

Fig. S4. SDS-PAGE and Western blot of GST, GST-FLV2, and GST-FLV4 proteins. Purified recombinant proteins (0.1 μg each) were analyzed by SDS–PAGE; the gel was stained with CBB. GST, GST-FLV2, and GST-FLV4 proteins were detected by the GST-antibody in Western-blots. Expected sizes of recombinant proteins are 26 kDa (GST), 92 (= 26 + 66) kDa (GST-FLV2), and 90 (= 26 + 64) kDa (GST-FLV4).

Figure S4. Shimakawa *et al*. (2014)

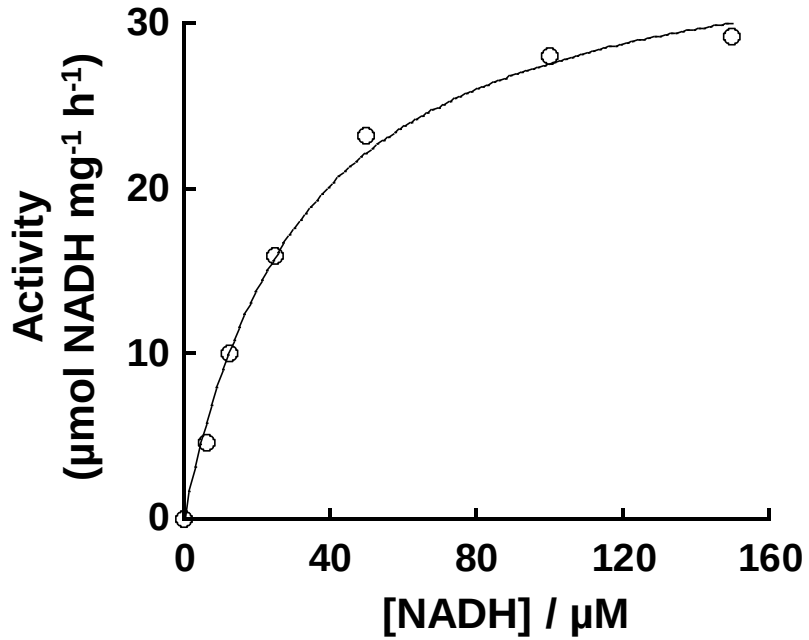

Fig. S5. Dependence of the NADH-oxidation activity on the concentration of NADH in the reaction catalyzed by the recombinant GST-FLV4 protein.

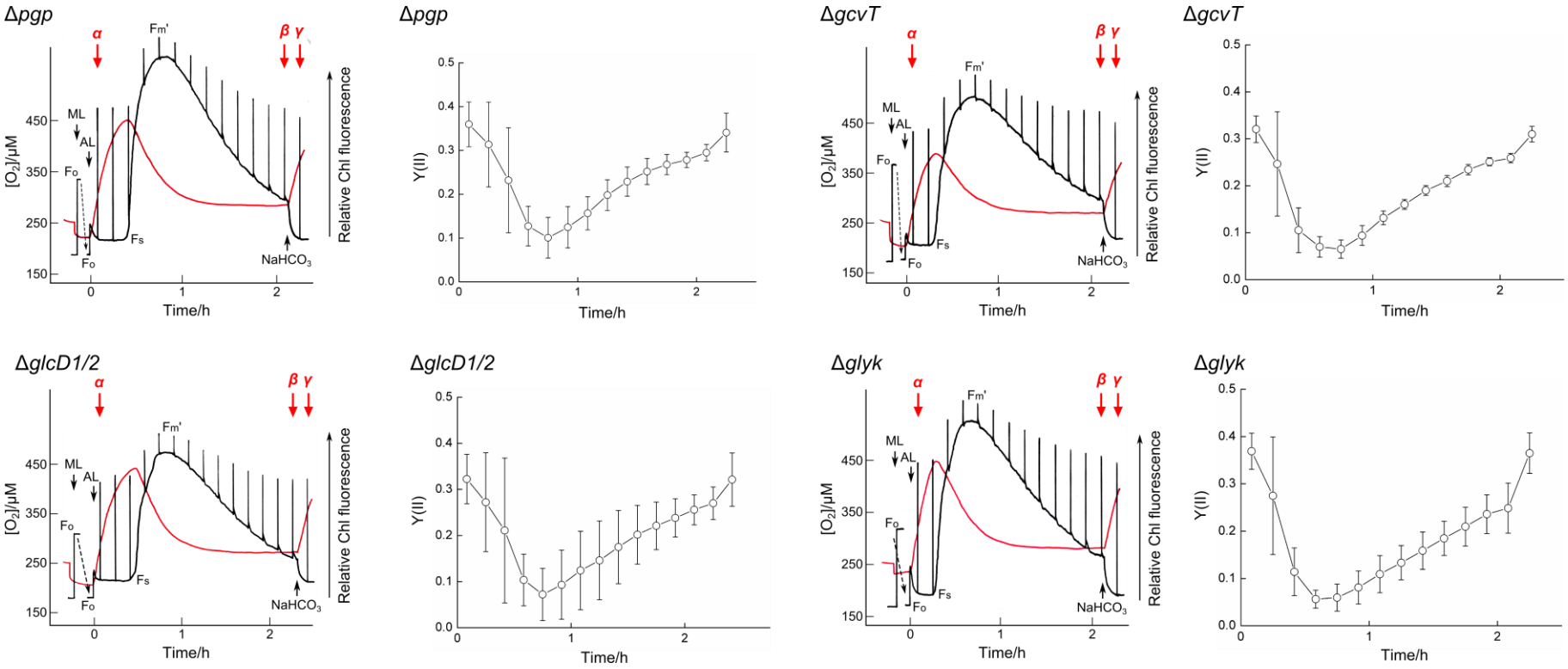

Fig. S6. Development of photosynthetic parameters in media containing four high-[CO_2]-grown deletion mutants of *S.* 6803, Δ*pgp* (top left), Δ*glcD1/2* (bottom left), Δ*gcvT* (top right), and Δ*glyk* (bottom right). Other details as in Fig. 1.

Figure S6. Shimakawa *et al.* (2014)